Available online at www.sciencedirect.com
ScienceDirect
Ceramics International 36 (2010) 1615–1619
CERAMICS INTERNATIONAL
www.elsevier.com/locate/ceramint

# Fabrication of $Sn^{4+}$ doped $Ba(Mg_{1/3}Ta_{2/3})O_3$ transparent ceramics by a solid state reaction method

Yihua Huang [a,b], Dongliang Jiang [a,*], Jingxian Zhang [a], Qingling Lin [a]

[a] The State Key Laboratory of High Performance Ceramics and Superfine Structure, Shanghai Institute of Ceramics, Shanghai 200050, China
[b] Graduate University of the Chinese Academy of Sciences, Beijing 100049, China

Received 19 September 2009; received in revised form 15 December 2009; accepted 20 February 2010

## Abstract

Transparent disordered BMT ceramics were obtained by solid state reaction. $Sn^{4+}$ ions were incorporated to make the B site of the perovskite structure disordered. The stoichiometric powder mixture with and without Sn doping was calcinated at 1300 °C, respectively and they were both characterized. After dry pressing, the pellets with Sn doping were sintered at 1600 °C in oxygen atmosphere for 4 h. The grain size of the transparent ceramics is around 12 μm. No pores were detected in or among the grains. The inline transmittance of the material is 66% at 580 nm. The refractive index is 2.09 at 1600 nm.

*Keywords:* A. Powders: solid state reaction; Sintering; C. Optical properties

## 1. Introduction

Ordered $Ba(Mg_{1/3}Ta_{2/3})O_3$ (abbreviated as BMT) was one of the most important microwave dielectric materials [1] because of its highest $Q$ value and higher dielectric constant among microwave materials. Recently disordered transparent BMT ceramic was reported [2] to be an excellent optical material, but no detail information is available.

BMT [3] is one of the order–disorder perovskite-type oxide compounds like barium zinc tantalite (BZT). While pure barium zinc niobate (BZN) [3] has a disordered perovskite structure. When disordered, they have cubic unit cells with $a_0 = 0.4095$ nm and $Pm3m$ symmetry. The ordered compounds adopt a trigonal symmetry owing to a rhombohedral distortion along a [1 1 1] direction of the cubic cell (shown in Fig. 1).

Cubic phase is one of the basic requirements for making transparent ceramics, such as $MgAl_2O_4$ [4], $Y_2O_3$ [5], YAG [6] and so on. Though alumina ceramic can be fully densified now, it is still translucent [7] due to its birefringence resulting from the intrinsic hexagonal structure.

Only if the optical axes of the hexagonal phase are oriented to be parallel to each other, alumina will be transparency [8]. So in order to produce transparent ceramic, it is better to obtain disorder perovskite-type BMT.

To make BMT disordered or ordered completely is not an easy task. The size and valency of B site ions [3] from $A(B'B'')O_3$ are the main factors that determine the ordered or disordered structure. If the difference between B′ and B″ in size and valency is small, it is disordered, like BZN ($Zn^{2+}$ and $Nb^{5+}$ seen in Table 1). In nature, the radius of some ions are similar, like $Ba^{2+}$, $Pb^{2+}$ and $La^{3+}$ for 12 coordination number, or $Mg^{2+}$, $Ta^{5+}$, $Sn^{4+}$, $Nb^{5+}$, $Zn^{2+}$ and $Zr^{4+}$ for 6 coordination number (shown in Table 1) [9]. These kinds of ions always substitute each other to form isomorphism, like PLZT [10], BLZN [11]. PLZT [10] is another interesting pseudo-cubic phase perovskite-type transparent ceramic. $Pb^{2+}$ ion has the similar size of ion radium to $La^{3+}$ ion. When $La^{3+}$ ion is doped, PZT phase is transformed from tetragonal to fake cubic phase. With the increase of $La^{3+}$ ion content, the optical birefringence of PLZT transparent ceramic deceases correspondingly [12], and the inline transmittance increases. In this paper we choose $Sn^{4+}$ ion with ion radium of 0.69 Å, which is just between the ion radium of $Mg^{2+}$ and $Ta^{5+}$. The $Sn^{4+}$ ion is used to reduce the difference between $Mg^{2+}$ ion and $Ta^{5+}$ ion both in ion radium and valency. Then disordered transparent BMT ceramics can be fabricated.

---

* Corresponding author. Tel.: +86 21 5241 2606; fax: +86 21 5241 3122.
*E-mail address:* withuyu@163.com (D. Jiang).

0272-8842/$36.00
doi:10.1016/j.ceramint.2010.02.041

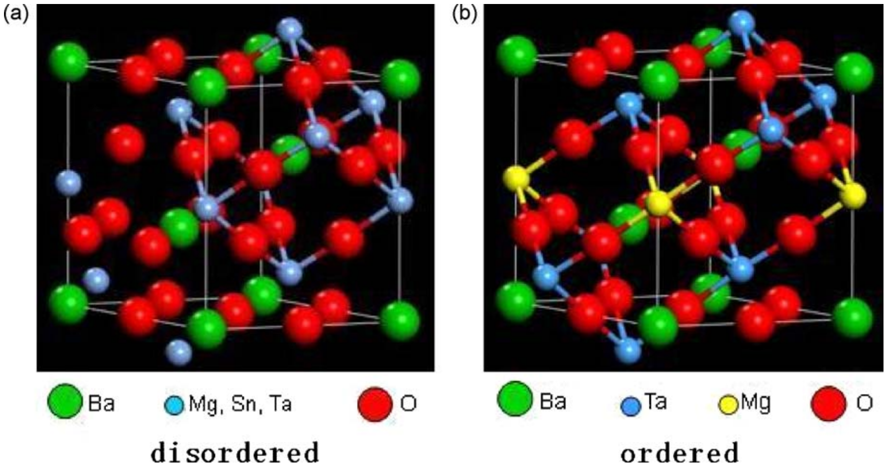

Fig. 1. Lattice structure of the disordered (a) and ordered (b) BMT.

Table 1
Ion radium (Å).

| Coordination number (CN) | $Ba^{2+}$ | $Pb^{2+}$ | $La^{3+}$ | $Mg^{2+}$ | $Ta^{5+}$ | $Sn^{4+}$ | $Nb^{5+}$ | $Zn^{2+}$ | $Zr^{4+}$ |
|---|---|---|---|---|---|---|---|---|---|
| VI | | | | 0.72 | 0.64 | 0.69 | 0.64 | 0.74 | 0.72 |
| XII | 1.61 | 1.49 | 1.36 | | | | | | |

## 2. Experiment procedure

### 2.1. Starting materials

Commercial barium carbonate and magnesium carbonate powder (Tianjin Guangfu Fine Chemical Research Institute, China, 99.99% purity), and a commercial tantalum oxide (CongHua tantalum & Niobium Smeltery, China, 99.99% purity) with a surface area of 6.61 $m^2/g$ were used as the starting materials. $SnO_2$ (Tianjin Guangfu Fine Chemical Research Institute, China, 99.99% purity) was added as sintering additive and one of the components.

### 2.2. Production processing

The starting powders with the stoichiometric ratio of BMT and some $SnO_2$ (10 at% of B site) were first ball-milled in a polyethylene bottle with zirconia balls in alcohol for 48 h. Then the alcohol was removed by drying the milled slurry at 80 °C for 24 h in an oven. The dried powder mixture was ground and sieved through 200 mesh screen. Then the powder mixture was calcinated at 800, 1000, 1100, 1200 and 1300 °C in flowing oxygen for 4 h. The calcinated powders were dry pressed into φ20 mm pellets in a steel mold and then cold isostatically pressed at 250 MPa. The pellets were then sintered at 1600 °C in oxygen atmosphere for 4 h. The sintered samples were ground and polished to transparent pellets. The polished surface was thermal etched at 1500 °C in oxygen atmosphere for 2 h.

### 2.3. Characterization

Differential thermal analysis (TG/DTA) of the mixture powder was conducted using a TG/DTA analyzer (Netzsch, Germany). The calcinated powders were analyzed by X-ray diffraction (Model D/MAX-2550 V, Rigaku, Japan), and the microstructures were observed by transmission electron microscope (JEM-200CX, JEOL, Tokyo, Japan). BET was used to obtain the specific surface area of calcinated powders. Surface and fracture surface microstructures of the specimens were observed by EPMA (Model JXA-8100, JEOL, Japan), while mirror-polished surface was thermal etched at 1500 °C for 2 h in alumina crucible. The grain sizes were measured by the linear-intercept method and calculated from $G = 1.5L$, where $G$ is the average grain size and $L$ is the average intercept length. Mirror-polished samples on both surfaces were used to measure the optical transmittance (Model U-2800 Spectrophotometer, Hitachi, Japan). Spectroscopic phase modulated ellipsometry (UVISEE/460VISA-GAS, JOBIN YVON) was used to detect the refractive indices of transparent ceramics.

## 3. Results and discussion

TG/DTA curves (Fig. 2) of the mixture powder show three endothermic peaks up to 1200 °C, with a total weight loss of 15.6%. This weight loss is very close to that of the theoretical calculation (15.46%) of the mixture powder with a composition of $[BaCO_3]$ $0.1[SnO_2]$ $0.3[MgCO_3]$ $0.3[Ta_2O_5]$. The first endothermic peak, located at about 412 °C, is caused by the decomposition of $MgCO_3$, meanwhile the mass loss is 4.4%, similar to the theoretical value. The second endothermic peak is located at about 828 °C. It is caused by the decomposition of $BaCO_3$ and by the formation of BMT and other phases [13]. The BMT phase can be detected on the XRD curves in Fig. 3, when the temperature is higher than 800 °C. The third endothermic peak [14] in Fig. 2, at about 1090 °C, may be caused by the

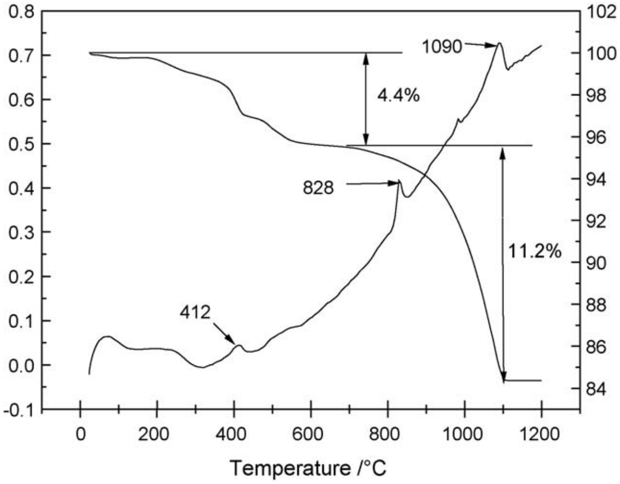

Fig. 2. TG/DTA curves of the mixture powder (10 °C/min).

transformation from satellite phases (like $Ba_4Ta_2O_9$ and $Ba_5Ta_4O_{15}$) to BMT phase.

The XRD results (Fig. 3) reveal that the crystallization of the mixture powder started between 800 and 1000 °C, at which point the $Ba_4Ta_2O_9$, $Ba_5Ta_4O_{15}$ and BMT phases were presented [15], corresponding to the TG/TDA observation. When calcined at 1200 °C, it resulted in an almost-complete phase conversion to BMT, and only a very small amount of satellite phase remained. The powder mixture was completely transformed to BMT at 1300 °C.

It is difficult to obtain pure ordered perovskite-type or disordered type. Most frequently, it is in the intermediate of the disorder-order type [3]. Many works have been done to make an ordered structure [15–17]. Fig. 4 shows the XRD spectra of BMT with and without Sn doping. The XRD results of BMT with Sn show cubic (or pseudo-cubic) phase with the space group as *Pm*3*m* (JCPDS No. 65-3240). And BMT without Sn show some kind of hexagonal phase (JCPDS No. 29-0203). When Sn is added, the order–disorder perovskite-type of BMT will tend to be disordered. In Fig. 1(b), the lattice structure of BMT is ordered. When Sn with similar properties like $Ta^{5+}$ and $Mg^{2+}$ is added Fig. 4(a), the lattice structure transformed to be disordered. For ordered sample, it is hexagonal phase. Much weak peaks will appear on the XRD curves compared to that of the disordered pseudo-cubic phase. This is due to the lattice distortion, which makes some coincident crystal planes differed. Planes (1 1 0), (1 0 1) and (0 1 1) of pseudo-cubic phase BMT are coincide (only (1 1 0) peak) on the XRD curves, but they show (1 1 0) and (1 0 1) peaks when it transforms to hexagonal phase. *S* parameter [18] is used to evaluate the cation ordering:

$$S = \sqrt{\frac{(I_{1\,0\,0}/I_{1\,1\,0})_{\text{obs}}}{(I_{1\,0\,0}/I_{1\,1\,0})_{\text{ord}}}}$$

where the theoretical value of completely ordered structure ($I_{1\,0\,0}/I_{1\,1\,0}$) is 8.14%, the less value *S* is, the more disordered the samples will be. In Fig. 4, the *S* value of BMT with Sn is 0.30, the *S* value without Sn is 0.76, which means that the addition of Sn can lead to a more disordered structure.

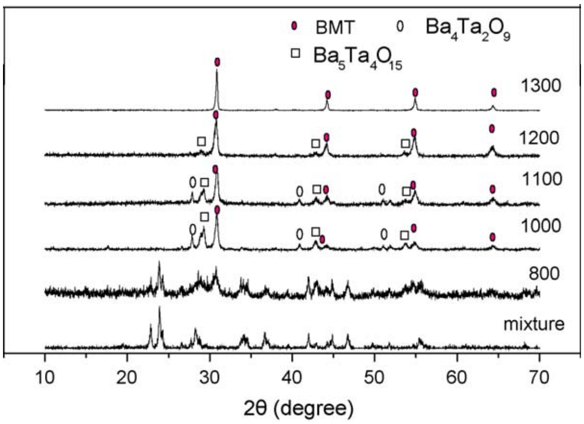

Fig. 3. XRD spectra of the powders calcined at different temperatures.

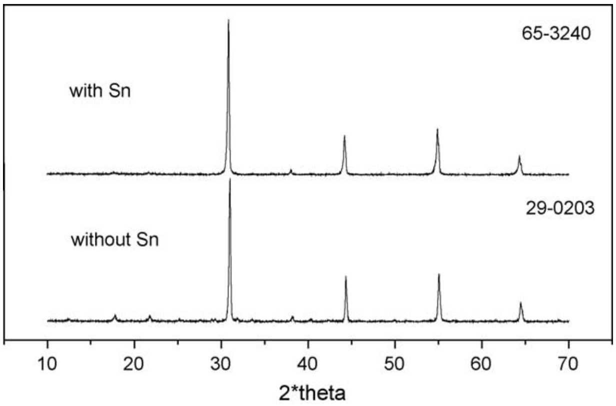

Fig. 4. XRD spectra of BMT powder with and without Sn doping.

The TEM photograph of the as-synthesised Sn doped BMT powder after calcinations at 1300 °C for 4 h is shown in Fig. 5. The crystalline size is about 40 nm. BET results show that the

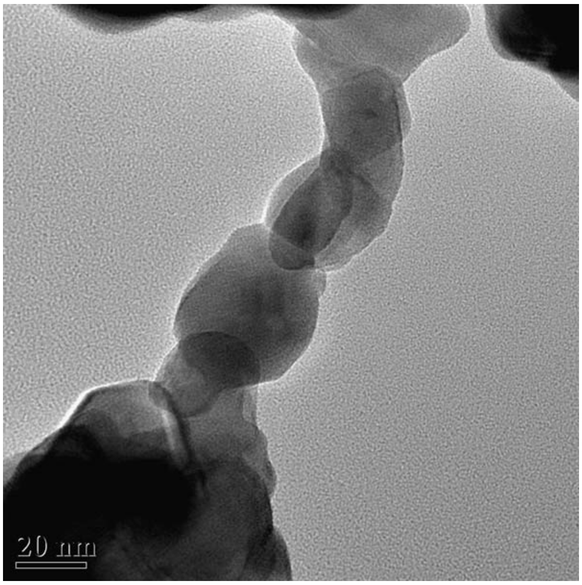

Fig. 5. TEM photographs of the mixture powder after calcinations at 1300 °C for 4 h.

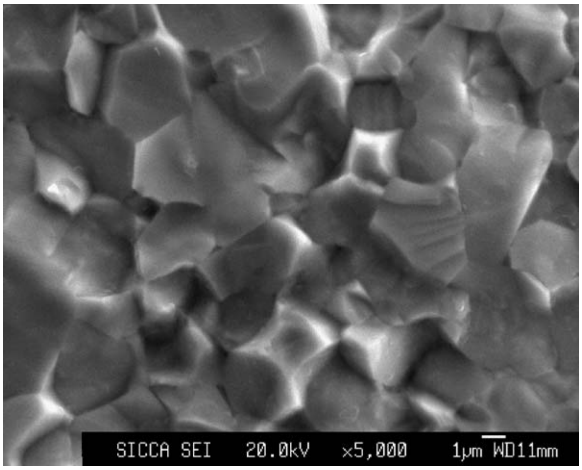

Fig. 6. The EPMA photograph of the fracture surface of Sn doped BMT ceramic after sintering at 1600 °C in oxygen atmosphere for 4 h.

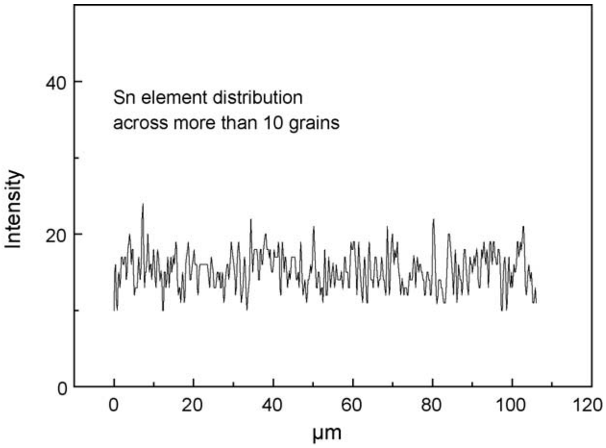

Fig. 8. Sn element distribution spectra in more than 10 grains by element line scan.

specific surface area of the powder is 2.5 $m^2$/g. The $D_{BET}$ (powder size calculated by specific surface) is estimated to be about 330 nm, which provide enough energy for sintering. The difference between the crystalline size and $D_{BET}$ was caused by the particle consolidation.

Fig. 6 shows the EPMA microstructure of the fracture surface of Sn doped BMT ceramic after sintering at 1600 °C for 4 h. Some place of the fracture surface is smooth and some is rough. That means the fracture mode of this material is a combination of both transgranular and intergranular facture. No pores can be detected in or among the grains.

After sintered and thermal etched, the micrograph of the mirror-polished surfaces of the Sn doped BMT transparent ceramics is shown in Fig. 7. No abnormal grain growth was founed. The grain size is about $12 \pm 4$ µm. There are two phases on the micrograph. According to the results of EDS, the light color phase contains 12 at% of B site (see in Table 1) Sn doped BMT material (spectrum 1), while Ta and Mg contains 61 and 27 at%, respectively, by EDX detecting. The deep color phase is mainly composed of Ba, Al and O (spectrum 2), the ratio of Ba and Al is 1:2. It is proposed that the deep phase is mainly $BaAl_2O_4$ based on BaO–$Al_2O_3$ phase diagram [19]. It was developed during the thermal etching because alumina crucible might react with the sample. Fig. 8 shows the Sn element distribution between more than 10 grains. It is detected that Sn element was equally distributed both in grains and grain boundaries. The zigzag curve in Fig. 8 is mainly caused by the machine error.

Fig. 9 shows in-line transmittance ($I/I_0$) of the Sn doped BMT transparent ceramics after sintering at 1600 °C in oxygen atmosphere for 4 h. The sample was 0.5 mm thick. And the transmittance at 600 nm was 66%. While the BMT pellets without Sn doping just show translucent after the same operations. And pellets with Sn but sintered at air atmosphere are just translucent, also. This is because nitrogen and other gas cannot dissolve in the oxide freely like oxygen during the sintering progress. The pores cannot be eliminated clearly if it is sintered in air. And MgO and SnO would evaporate at high temperature if the oxygen partial pressure is not high enough. That would cause the appearance of vancancies which act as the scattering centers and lead to the decrease of the inline transmittance. The existence of pores and its partially ordered property would be the two main reasons to affect the transparency.

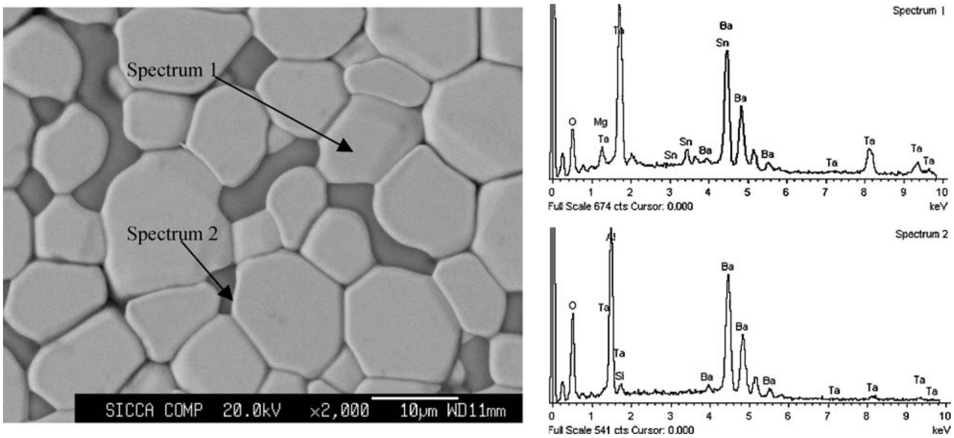

Fig. 7. The EPMA photograph and EDS analysis of the polished surface of Sn doped BMT ceramic after sintering at 1600 °C in oxygen atmosphere for 4 h and thermal etching.

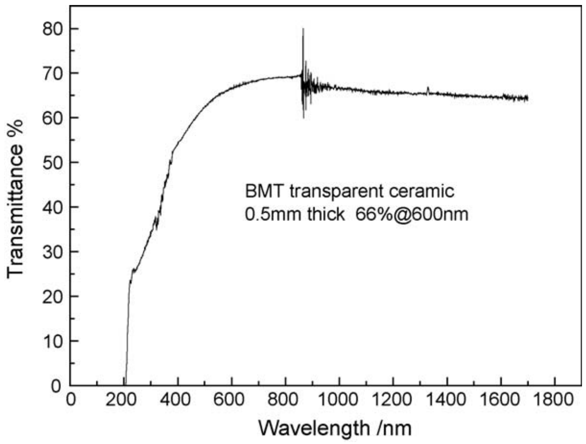

Fig. 9. Optical inline transmittance spectra of Sn doped BMT transparent ceramic at a thickness of 0.5 mm.

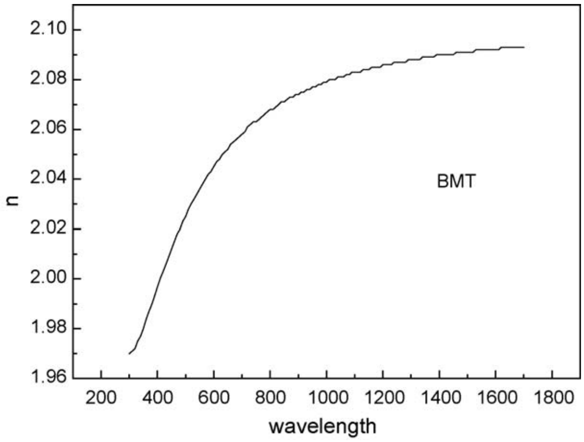

Fig. 10. The refractive indices of the Sn doped BMT ceramic.

Fig. 10 shows the refractive indices of the Sn doped BMT ceramic at different wavelength. Since Ta has a big atomic weight, the material has high refractive index, 2.09 at 1600 nm. The refractive indices increase with the increasing of the wavelength, which is very interesting.

## 4. Conclusions

(1) Perovskite-type BMT ceramic can be transparent if it shows disordered pseudo-cubic phase.
(2) $Sn^{4+}$ ion can substitute $Mg^{2+}$ and $Ta^{5+}$ in B site, and make the perovskite-type disordered.
(3) Sn doped BMT transparent ceramic is obtained after sintering in oxygen atmosphere at 1600 °C for 4 h, while the BMT ceramic without Sn doping is only translucent after all the same operations.

## Acknowledgements

This work was supported by the National Natural Science Foundation of China (no. 50772128), Shanghai Science and Technology Committee (nos. 07DJ14001, 07pj14094), and the State Key Laboratory of High Performance Ceramics and Superfine Microstructures.

## References

[1] Y. Fang, A. Hu, S. Ouyang, J. Oh, The effect of calcination on the microwave dielectric properties of $Ba(Mg_{1/3}Ta_{2/3})O_3$, J. Eur. Ceram. Soc. 21 (15) (2001) 2745–2750.
[2] N. Tanaka, Y. Higuchi, M. Katsube, M. Sube, Transparent ceramic comprises one of three specific formulae, and has specified refractive index and ferroelectric properties, Patent No. CN1424990-A.
[3] D. Barber, K. Moulding, J. Zhou, M. Li, Structural order in $Ba(Zn_{1/3}Ta_{2/3})O_3$, $Ba(Zn_{1/3}Nb_{2/3})O_3$ and $Ba(Mg_{1/3}Ta_{2/3})O_3$ microwave dielectric ceramics, J. Mater. Sci. 32 (6) (1997) 1531–1544.
[4] K. Morita, B. Kim, K. Hiraga, H. Yoshida, Fabrication of transparent $MgAl_2O_4$ spinel polycrystal by spark plasma sintering processing, Scripta Mater. 58 (12) (2008) 1114–1117.
[5] J. Zhang, L. An, M. Liu, S. Shimai, S. Wang, Sintering of Yb3+: $Y_2O_3$ transparent ceramics in hydrogen atmosphere, J. Eur. Ceram. Soc. 29 (2) (2009) 305–309.
[6] T. Tachiwaki, M. Yoshinaka, K. Hirota, T. Ikegami, O. Yamaguchi, Novel synthesis of $Y_3Al_5O_{12}$ (YAG) leading to transparent ceramics, Solid State Commun. 119 (10–11) (2001) 603–606.
[7] K.O. Hiroyuki Mizuta, Y. Shibasaki, M. Maeda, M. Machida, K. Ohshima, Preparation of high-strength and translucent alumina by hot isostatic pressing, J. Am. Ceram. Soc. 75 (2) (1992) 469–473.
[8] S. Wang, X. Mao, S. Shimai, J. Guo, Transparent polycrystalline alumina ceramics with orientated optical axes, J. Am. Ceram. Soc. 91 (10) (2008) 3431–3433.
[9] K. Cvetkovic, A. Petric, Periodic table of the oxides, Am. Ceram. Soc. Bull. 79 (4) (2000) 65–69.
[10] G.S. Snow, Fabrication of transparent electooptic PLZT ceramics by atmosphere sintering, J. Am. Ceram. Soc. 56 (2) (1973) 91–96.
[11] C. Lee, Y. Lin, C. Huang, C. Su, C. Hu, Structural and dielectric characteristics of barium lanthanum zinc niobate, J. Am. Ceram. Soc. 89 (12) (2006) 3662–3668.
[12] P. Chou, J. Zheng, W. Cheng, X. He, A. Ding, Preparation and properties of transparent ferroelectic PLZT (x/65/35) ceramics, J. Funct. Mater. 35 (1) (2004) 1522–1524.
[13] C.H. Lu, C.C. Tsai, Reaction kinetics, sintering characteristics, and ordering behavior of microwave dielectrics: barium magnesium tantalate, J. Mater. Res. 11 (5) (1996) 1219–1227.
[14] J.J. Bian, M.Y. Zhao, Z.W. Yin, Synthesizing process and sinterability of $Ba(Mg_{1/3}Ta_{2/3})O_3$, J. Inorg. Mater. 13 (5) (1998) 710–714.
[15] X. Chen, Y. Suzuki, N. Sato, Sinterability improvement of $Ba(Mg_{1/3}Ta_{2/3})O_3$ dielectric ceramics, J. Mater. Sci-Mater. Electron. 5 (4) (1994) 244–247.
[16] O. Renoult, J.P. Boilot, F. Chaput, R. Papiernik, L.G. Hubertpflalzgraf, M. Lejeune, Sol–gel processing and microwave characteristics of $Ba(Mg_{1/3}Ta_{2/3})O_3$ dielectrics, J. Am. Ceram. Soc. 75 (12) (1992) 3337–3340.
[17] K. Surendran, P. Mohanan, M. Sebastian, The effect of glass additives on the microwave dielectric properties of $Ba(Mg_{1/3}Ta_{2/3})O_3$ ceramics, J. Solid State Chem. 177 (2004) 4031–4046.
[18] K. Surendran, M. Sebastian, P. Mohanan, R. Moreira, A. Dias, Effect of nonstoichiometry on the structure and microwave dielectric properties of $Ba(Mg_{0.33}Ta_{0.67})O_3$, Chem. Mater. 17 (1) (2005) 142–151.
[19] X. Ye, W. Zhuang, C. Deng, W. Yuan, Z. Qiao, Thermodynamic investigation on the $Al_2O_3$–BaO binary system, Calphad 30 (3) (2006) 349–353.